

## Influence of Deposition Temperature and Pressure on Microstructure and Tribological Properties of Arc Ion Plated Ag Films

HU Ming<sup>1,2</sup>, GAO Xiaoming<sup>1</sup>, SUN Jiayi<sup>1</sup>, WENG Lijun<sup>1</sup>, ZHOU Feng<sup>1</sup>, and LIU Weimin<sup>1,\*</sup>

*1 State Key Laboratory of Solid Lubrication, Lanzhou Institute of Chemical Physics,  
Chinese Academy of Sciences, Lanzhou 730000, China*

*2 Graduate School of Chinese Academy of Sciences, Beijing 100039, China*

Received May 13, 2011; revised November 23, 2011; accepted November 30, 2011

**Abstract:** The films deposited at low temperature (LT-films) have increasingly attracted theoretical and technical interests since such films exhibit obvious difference in structure and performances compared to those deposited at room temperature. Studies on the tribological properties of LT-films are rarely reported in available literatures. In this paper, the structure, morphology and tribological properties of Ag films, deposited at LT (166 K) under various Ar pressures on AISI 440C steel substrates by arc ion plating (AIP), are studied by X-ray diffraction (XRD), atomic force microscopy (AFM) and a vacuum ball-on-disk tribometer, and compared with the Ag films deposited at RT (300 K). XRD results show that (200) preferred orientation of the films is promoted at LT and low Ar pressure. The Crystallite sizes are 70 nm–80 nm for LT-Ag films deposited at 0.2 Pa and 0.8 Pa and larger than 100 nm for LT-Ag films deposited at 0.4 Pa and 0.6 Pa, while they are 55 nm–60 nm for RT-Ag films deposited at 0.2 Pa–0.6 Pa and 37 nm for RT-Ag films deposited at 0.8 Pa. The surfaces of LT-Ag films are fibre-like at 0.6 Pa and 0.8 Pa, terrace-like at 0.4 Pa, and sphere-like at 0.2 Pa, while the surfaces of RT-Ag films are composed of sphere-like grains separated by voids. Wear tests reveal that, due to the compact microstructure LT-Ag films have better wear resistances than RT-Ag film. These results indicate that the microstructure and wear resistance of Ag films deposited by AIP can be improved by low temperature deposition.

**Key words:** low temperature; Ag films; structure; tribological properties

### 1 Introduction

Due to the property of low shear strength, Ag films have been widely used as solid lubricant to reduce friction and wear on contact surfaces of moving mechanical components in space environment<sup>[1]</sup>. The friction and wear performances of physical vapor deposited (PVD) Ag films are strongly dependent on its structure such as morphology<sup>[2]</sup>, preferred orientation<sup>[3]</sup> and grain size<sup>[4]</sup>, which is influenced significantly by deposition parameters such as substrate temperature<sup>[5]</sup> and gas pressure<sup>[6]</sup> etc. Therefore, to optimize deposition parameters of Ag films is of vital importance for obtaining desirable tribological properties.

In recent years, the films deposited at low temperature (LT) have increasingly attracted theoretical and technical interests since such films exhibit obvious difference in structure and performances compared to those deposited at room temperature (RT)<sup>[7–14]</sup>. Sputtered Ni films at liquid nitrogen temperature and low Ar pressure showed excellent

(111) orientation and good crystallinity<sup>[7]</sup>. Ti70-Al30 films deposited at liquid nitrogen temperature exhibited dense nanocrystalline structure, whereas RT-films showed voids and discontinuities in their columnar grain morphology<sup>[8]</sup>. Fe films deposited at liquid nitrogen temperature had better crystallinity and much smaller coercive force than RT-Fe films<sup>[9]</sup>. The resistivity value of Au films deposited at liquid nitrogen temperature was more than four orders lower than that of RT-Au film<sup>[10]</sup>. The nucleation and growth mode of Ag films deposited at LT during the initial stage of film deposition were studied<sup>[15–19]</sup>. The thickness of soft metal films used as lubricant normally has to be much thicker than 100 nm<sup>[20]</sup>. The structure and tribological properties of Ag films were influenced by film thickness<sup>[20–21]</sup>. Our previous study<sup>[22]</sup> reported the effects of substrate temperature (130–217 K) and bias voltage on the preferred orientation and tribological properties of Ag films with a thickness of 646–838 nm, but the morphology of such LT-Ag films and its relationship with tribological properties were still uncovered. Further, the gas pressure effects on the structure and properties of LT-Ag films have been little reported.

In this paper, Ag films are deposited on AISI 440C steel substrates at LT (166 K) under various Ar pressures by an AIP system. The effects of Ar pressure on the structure

\* Corresponding author. E-mail: wmliu@licp.cas.cn

This project is supported by National Basic Research Program of China (973 Project, Grant No.2007CB607601), and National Natural Science Foundation of China (Grant No. 50301015)

and tribological properties of LT-Ag films are investigated and compared with RT-Ag films.

## 2 Film Deposition and Characterization Experiment

### 2.1 Film deposition

Ag films are deposited on AISI 440C steel substrates (HRC 60, 25 mm × 25 mm × 5 mm) at 166 K (LT) and 300 K (RT) under Ar pressures of 0.2 Pa, 0.4 Pa, 0.6 Pa and 0.8 Pa by an AIP system with a sample holder cooled by liquid nitrogen, as illustrated in Fig. 1. A cylindrical Ag target with a purity of 99.95 wt. % and a diameter of 80 mm is used as arc cathode, and its surface is parallel to substrate surfaces. The distances between the target and substrates are 300 mm–318 mm. The substrates are surface-polished with abrasive paper, followed ultrasonically cleaned with acetone for 20 min, and then fixed on the sample holder surface. The surface roughness ( $R_a$ ) of polished substrates is  $0.06 \mu\text{m} \pm 0.02 \mu\text{m}$ , measured by a NanoMap 500LS three-dimensional (3D) profilometer with a stylus tip in tapping mode. Substrate temperatures are measured by platinum resistors attached to the back of the substrates.

Before deposition, the vacuum chamber is evacuated to a background vacuum below  $6.0 \times 10^{-3}$  Pa. The substrates are Ar ion etched at a bias of 800 V for 10 min, and then cooled by piping liquid nitrogen into the sample holder to desired temperatures. Detailed deposition parameters are listed in Table 1.

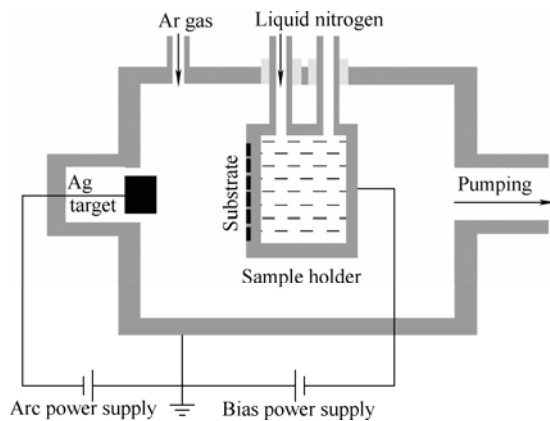


Fig. 1. Schematic illustration of the AIP system

Table 1. Film deposition parameters

Parameter	Value
Ar pressure $p/\text{Pa}$	0.2, 0.4, 0.6, 0.8
Substrate temperature $T_s/\text{K}$	166, 300
Substrate bias voltage $V_B/\text{V}$	800
Arc current $I_A/\text{A}$	80
Deposition duration $t/\text{min}$	10
Film thickness $\delta/\text{nm}$	600–650

### 2.2 Structure and properties characterization

The structure of the films is analyzed by an X-ray diffraction (XRD, Philips X'Pert Pro) with  $\theta/2\theta$  scanning

pattern using Cu  $K\alpha$  radiation ( $\lambda=1.5406 \text{ \AA}$ ). The surface morphology is observed by an atomic force microscope (AFM, Nanoscope III). The friction and wear tests are performed by a vacuum ball-on-disk tribometer. The disks are the Ag films coated steel substrates. AISI 440C steel balls (HRC 60,  $R_a 0.10 \mu\text{m}$ ) with a diameter of 8 mm are used as counterparts and cleaned with alcohol before each test. Test conditions: normal load of 2 N, rotational speed of 400 r/min, RT, and ambient vacuum  $< 5 \times 10^{-3}$  Pa. The wear tracks are analyzed by a scanning electron microscope (SEM, JSM-5600LV) coupled with an energy dispersive X-ray spectrometer (EDS, KEVEX). The wear volume loss is evaluated by a NanoMap 500LS three-dimensional (3D) profilometer with a stylus tip in tapping mode. The wear rates ( $K$ ) are calculated using the equation of  $K=V/(F \cdot S)^{-1}$ , where  $V$  is the wear volume loss in  $\text{mm}^3$ ,  $F$  the normal load applied in N, and  $S$  the sliding distance in m.

## 3 Results and Discussion

### 3.1 Structure

Fig. 2 (a) and Fig. 2 (b) exhibit the XRD patterns of LT- and RT-Ag films deposited under various Ar pressures. LT-Ag films show both (111) and (200) peaks, and the relative intensity of (200) peak is increased with decreasing Ar pressure. As the Ar pressure is decreased to 0.2 Pa, almost only (200) peak is observed, indicating an excellent (200) preferred orientation. The relative intensity of (200) peaks of RT-Ag films is lower than that of LT-Ag films and also shows a tendency to increase with decreasing Ar pressure. These results indicate that the films mainly show two types of grain orientation: (111) or (200) plane parallel to the substrate surface, and the latter is advanced at LT and lower Ar pressure.

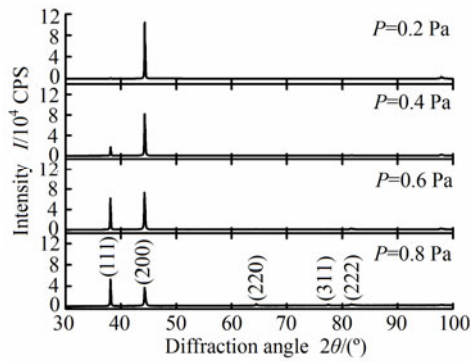
Preferred orientation degree of the films ( $P(hkl)$ ) can be calculated by Eq. (1)<sup>[22]</sup> and the calculated (200) preferred orientation degree ( $P(200)$ ) of both LT- and RT-Ag films is shown in Fig. 3. It can be seen that as the Ar pressure decreases from 0.8 Pa to 0.2 Pa, the  $P(200)$  of LT- and RT-Ag films increases from 1.21 to 1.99 and 0.97 to 1.34, respectively. This indicates that RT-Ag film deposited at 0.8 Pa shows a much poor (111) preferred orientation ( $P(200)=0.97 < 1$ ), other films exhibit (200) preferred orientation ( $P(200) > 1$ ) and the  $P(200)$  is promoted at LT and low Ar pressure. Especially for LT-Ag film deposited at 0.2 Pa, the  $P(200)$  is close to 2.0, indicating an excellent (200) preferred orientation.

$$P(hkl)_i = \frac{I(hkl)_i}{I_0(hkl)_i} \left[ \frac{1}{n} \sum_{i=1}^n \frac{I(hkl)_i}{I_0(hkl)_i} \right]^{-1} \quad (1)$$

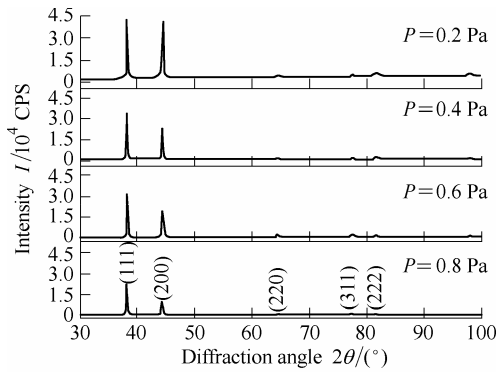
The average crystallite size can be estimated from the width at half maximum (FWHM) in the XRD pattern using Scherrer equation<sup>[22]</sup>:

$$D = K \lambda \cdot (\beta \cdot \cos \theta)^{-1}, \quad (2)$$

where  $D$  is the crystallite size (nm),  $K$  Scherrer constant (0.89),  $\lambda$  the X-ray wavelength (1.540 6 Å),  $\beta$  the FWHM, and  $\theta$  the diffraction angle. According to Eq. (2) and the FWHM of the (111) peaks in the XRD patterns, the crystallite sizes of the films are calculated. As shown in Fig. 4, the crystallite sizes are 70 nm–80 nm for LT-Ag films deposited at 0.2 Pa and 0.8 Pa. The crystallite sizes of LT-Ag films deposited at 0.4 Pa and 0.6 Pa exceed the calculation limit of Scherrer formula (<100 nm), indicating that they are larger than 100 nm. Compared to LT-Ag films, RT-Ag films show small crystallite sizes about 58 nm at 0.2 Pa–0.6 Pa and 37 nm at 0.8 Pa.



(a) LT-Ag films



(b) RT-Ag films

Fig. 2. XRD patterns of the LT- and RT-Ag films

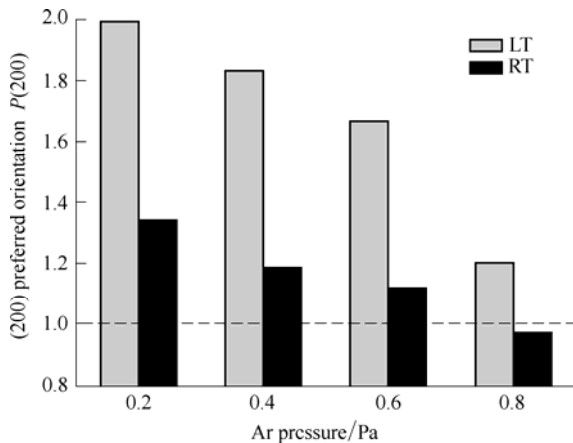


Fig. 3. (200) preferred orientation  $P(200)$  of the LT- and RT-Ag films

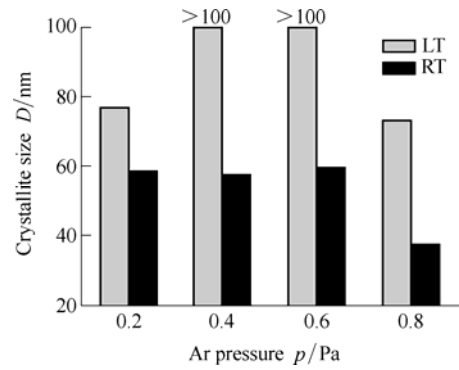
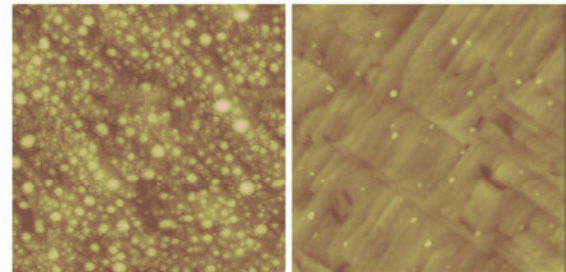


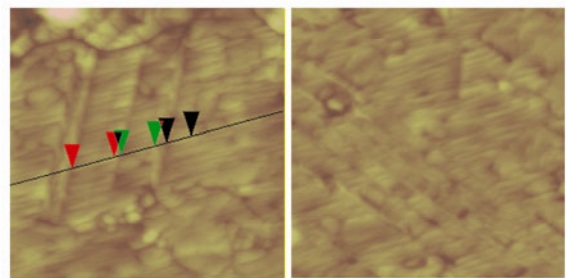
Fig. 4. Crystallite sizes of the RT- and LT-Ag films

Fig. 5(a–d) shows the AFM images of LT-Ag films deposited at various Ar pressures. Typical section analysis of the AFM image is shown in Fig. 5(e). It is evident that the surfaces of LT-Ag films are obviously influenced by the Ar pressure. The surfaces of LT-Ag films deposited at 0.6 Pa and 0.8 Pa are composed of fibre-like grains. The section analysis reveals that the fibre-like grains are oblique to the substrate surface. As the Ar pressure is decreased to 0.4 Pa, the film exhibits a terrace-like morphology. As the Ar pressure is further decreased to 0.2 Pa, the film surface shows a few sphere-like grains. AFM images of RT-Ag films are shown in Fig. 6. It can be seen that the surfaces of RT-Ag films are consisted of sphere-like grains separated by voids.



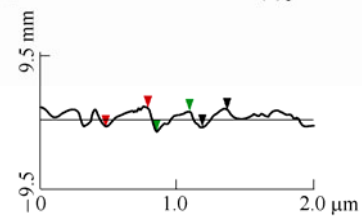
(a)  $p = 0.2$  Pa

(b)  $p = 0.4$  Pa



(c)  $p = 0.6$  Pa

(d)  $p = 0.8$  Pa



(e) Cross section profile along the line shown in Fig. 1 (c)

Fig. 5. AFM images of LT-Ag films and typical cross section profile (Image sizes are  $2.0 \times 2.0 \mu\text{m}^2$  in lateral and 20 nm full scale in height)

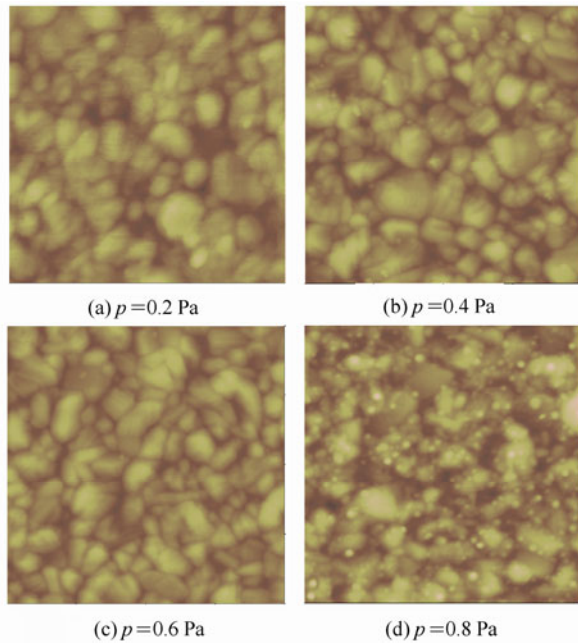


Fig. 6. AFM images of RT-Ag films (Image sizes are  $2.0 \mu\text{m} \times 2.0 \mu\text{m}$  in lateral and 30 nm full scale in height)

The structure of PVD polycrystalline metal films is strongly dependent on deposition parameters and described using a well-known structure zone model proposed by MOVCHAN and DEMCHISHIN<sup>[23]</sup> and developed by THORNTON<sup>[24]</sup>, BARNA, et al<sup>[25]</sup>, and ANDERS<sup>[26]</sup>. In this model, the film is characterized by different zones based on  $T_s/T_m$  ( $T_s$  is substrate temperature;  $T_m$  is melting point of metal). In zone I ( $0 < T_s/T_m < 0.2$ ), the film is composed of fibres which are growing uninterruptedly side by side. In zone T ( $0.2 < T_s/T_m < 0.4$ ), the film is composed of V-shaped grains with domed tops separated by voids. In Zone II ( $T_s/T_m > 0.4$ ) the film represents a homogeneous structure composed of columns penetrating from the bottom to the top of the film. In zone III, the film is characterized by equiaxed three dimensional grains. In present study, the surface features of LT-Ag films ( $T_s/T_m=0.13$ ) deposited at 0.6 and 0.8 Pa suggests a zone I structure composed of uninterrupted fibres, mainly attributed to the lack of both surface and bulk diffusions<sup>[25]</sup>. The fibres have been growing in a direction oblique to substrate surface and hence the upper of the fibres is exposed on film surface and resulted in such surface feature. As the Ar pressure decreases to 0.4 Pa, the fibres are connected to form a piece because of the improved mobility of deposition atoms, and so the film shows a terrace-like surface. Further decreasing Ar pressure to 0.2 Pa, the mobility of deposition atoms could be more remarkable, and so the film partially shows the surface features of zone T where the competitive grain growth results in V-shaped grains with domed tops separated by voids. The surface features of RT-Ag films ( $T_s/T_m=0.24$ ) are typical for metal films in zone T due to the higher substrate temperature. The difference, that the growth of the fibre-like grains of LT-Ag films is uninterrupted while

the growth of V-shaped grains of the RT-Ag films is interrupted, results in LT-Ag films with larger grain sizes than RT-Ag film.

The preferential orientation of the films is a result of competition between the surface and strain energies, and the growing film develops into a crystallographic structure with minimum total system energy. For the fcc Ag crystal, (111) plane has the lowest surface energy, while (200) plane has the lowest strain energy<sup>[27-28]</sup>. Due to the minimization of surface energy, the Ag films normally shows (111) preferred orientation<sup>[29]</sup>. However, in this study, the LT-Ag films show excellent (200) preferred orientation, especially at low Ar pressure. At LT, the surface diffusion of deposition atoms is much insufficient and so the orientation of nuclei becomes random<sup>[25]</sup>, resulting in accumulation of stress in the films. As the internal stress is accumulated enough, it would be released by strain, which induces reorientation of the crystallites. (200) plane of fcc Ag crystal have the lowest strain energy, so (200) orientation is preferred. The decrease in the  $P(200)$  with increasing Ar pressure is mainly attributed to the minimization of surface energy. The collision between the Ag and Ar ions is advanced by the increase in Ar pressure and simultaneously results in the energy loss of Ag ions<sup>[6]</sup>. As a result, the mobility of deposited Ag atoms at substrate surface is lowered. This is favored for growing of crystallites with (111) plane parallel to substrate surface due to (111) plane of fcc Ag crystal with the minimum surface energy, and hence the  $P(200)$  decreases with increasing Ar pressure.

### 3.2 Tribological properties

A vacuum ball-on-disk tribometer is used to evaluate the friction and wear of the Ag films. A typical sliding friction curve of the Ag film coated disk against steel ball is shown in Fig. 7. The friction curve of all the Ag films firstly shows a low and stable friction stage where the friction coefficient is at a range of 0.14–0.18. Afterwards, it exhibits a high and unstable friction stage with the mean friction coefficients of about 0.3, after which it shows a sudden increase in friction coefficient higher than 0.4, indicating the end of the film service life.

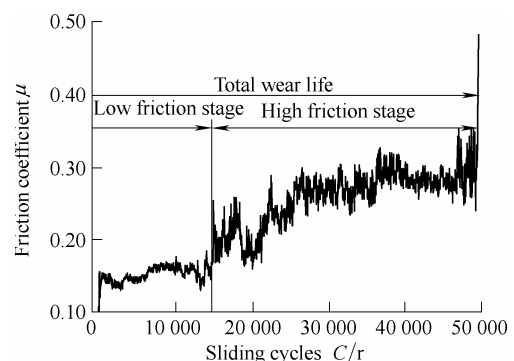


Fig. 7. Friction curve of Ag films deposited at LT and 0.6 Pa

After friction tests, the wear tracks on the Ag films coated substrate surfaces and corresponding wear scars on counterpart surfaces are observed by SEM. The element components of wear scars are also analyzed by EDS. Typical SEM and EDS results are shown in Fig. 8. It can be seen that after the low friction stage, the wear track is narrow and smooth, but the Ag film in the wear track region is almost exhausted and a great deal of wear debris can be observed on the wear scar surface. EDS result reveals that Ag content about 16.9 at. % is high at the wear scar area. It indicates that Ag transfer film is formed on the counterpart surface. After the total wear life, the wear track surface becomes relatively wide and the Ag transfer film is almost exhausted. These results indicate that at the low friction stage, the lubrication is provided by the Ag film and so the friction coefficient is low and stable. Meantime, the worn Ag gradually adheres to the counterpart surface to form a transfer film. As the Ag film is exhausted, the transfer film acts as a lubricating effect between the counterpart and bare substrate surfaces, but it will be insufficient at late stage, and hence the friction coefficient turns to high and unstable. As the lubricating effect of the transfer film fails, strong adhesive wear will occur between the bare substrate and counterpart surfaces, resulting in much high friction coefficient.

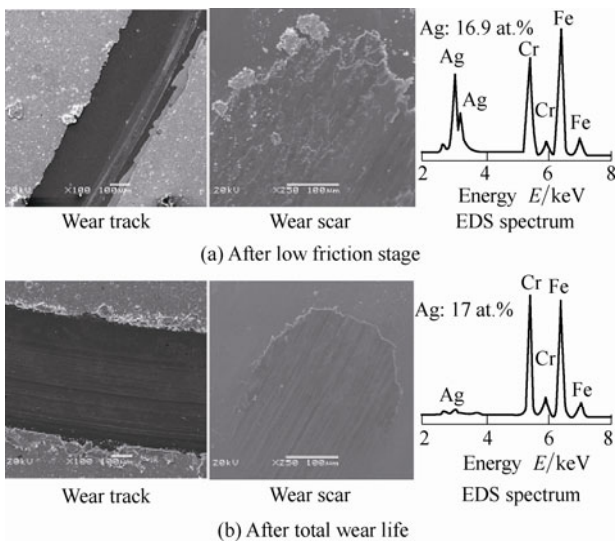


Fig. 8. Wear tracks of Ag film deposited at LT and 0.6 Pa, and the corresponding wear scars and EDS spectra from counterpart surfaces

Two sets of wear rates are calculated from the low friction stage and total wear life, respectively, shown in Fig. 9. The wear rates of LT-Ag films are lower than those of RT-Ag films and the wear rates of the total wear life are lower than those at low friction stage. At LT, the lowest wear rate is obtained from the film deposited at 0.4 Pa, while the highest wear rate is obtained from the film deposited at 0.2 Pa. At RT, the lowest and highest wear rates are obtained from the films deposited at 0.6 Pa and 0.2 Pa, respectively.

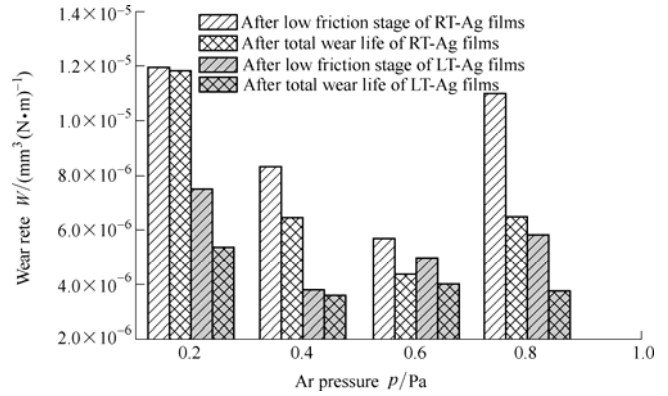


Fig. 9. Wear rates of the RT- and LT-Ag films

The changes in the wear rates with the substrate temperature and Ar pressure are correlated with the structure of the films. AFM results reveal that RT-Ag films shows a zone T structure, composed of V-shaped grains separated by voids, suggesting a loose film structure. At lower pressure, volume of the voids should become large because the surface diffusion is improved while the bulk diffusion is strongly limited<sup>[26]</sup>. Therefore, the wear rates are relatively high and the highest wear rate was obtained from the RT-Ag film deposited at 0.2 Pa. However, the LT-Ag films deposited at 0.4 Pa – 0.8 Pa shows zone I structure, composed of uninterrupted grown fibres side by side, and hence the voids in the films are suppressed. Correspondingly, the films are densified and show better wear resistances. LT-Ag film deposited at 0.2 Pa partially shows a zone T structure and so is accompanied with a relatively high wear. Furthermore, the wear rates of the total wear life being lower than those of the low friction stage indicates that the transfer films play an important role in reducing wear of the films. The wear rates of the low friction stage and total wear life show a similarly changed tendency with the Ar pressure, suggesting that better structure is also helpful for formation of the transfer film on the counterpart surface for further reduction of wear.

#### 4 Conclusions

(1) The preferred orientation of Ag films deposited by AIP can be significantly influenced by substrate temperature and Ar pressure, and the (200) preferred orientation is promoted at LT and low Ar pressure so an Ag film with excellent (200) preferred orientation is obtained at LT and 0.2 Pa.

(2) LT-Ag films mainly show a fibre-like grain structure, but it can be changed to V-shaped grain structure due to the decrease in Ar pressure or increase in substrate temperature.

(3) The wear resistance of Ag films is mainly dependent on the compactness of their structure. LT-Ag films show compacter structure and so better wear resistance than RT-Ag films.

## References

- [1] ROBERTS E W, TODD M J. Space and vacuum tribology[J]. *Wear*, 1990, 136(1): 157–167.
- [2] LEE K H, TAKAI O, LEE M H. Tribological and corrosive properties of silver thin films prepared by e-beam ion plating method[J]. *Surf. Coat. Technol.*, 2003, 169–170: 695–698.
- [3] GOTO M, AKIMOTO K, HONDA F. The effect of the crystallographic orientation of Ag thin films on their tribological performance[C]//*Proceedings of the 31st Leeds-Lyon Symposium on Tribology Held*, Trinity and All Saints College, Horsforth, Leeds, UK September 7–10, 2004: 667–672.
- [4] FLORES M, MUHL S, HUERTA L, et al. The influence of the period size on the corrosion and the wear abrasion resistance of TiN/Ti multilayers[J]. *Surf. Coat. Technol.*, 2005, 200(5–6): 1 315–1 319.
- [5] YANG F L, SOMEKH R E, GREER A L. UHV magnetron sputtering of silver films on rocksalt: quantitative X-ray texture analysis of substrate-temperature-dependent microstructure[J]. *Thin Solid Films*, 1998, 322(1–2): 46–55.
- [6] JUNG Y S. Study on texture evolution and properties of silver thin films prepared by sputtering deposition[J]. *App. Sur. Sci.*, 2004, 221(1–4): 281–287.
- [7] SHIMIZUA H, SUZUKIB E, HOSHI Y. Crystal orientation and microstructure of nickel film deposited at liquid nitrogen temperature by sputtering[J]. *Electrochim. Acta*, 1999, 44(21–22): 3 933–3 944.
- [8] KALE A, SEAL S, SOBCZAK N, et al. Effect of deposition temperature on the morphology, structure, surface chemistry and mechanical properties of magnetron sputtered Ti70-Al30 thin films on steel substrate[J]. *Surf. Coat. Technol.*, 2001, 141(2–3): 252–261.
- [9] WATARU S, YOICHI H, HIDEHIKO S. Fe and Fe–N films sputter deposited at liquid nitrogen Temperature[J]. *J. Magn. Magn. Mater.*, 2001, 235(1–3): 196–200.
- [10] HE L, SHI Z Q. Effect of deposition temperature on electric conduction and microstructure of Au films[J]. *Solid-State Electron.*, 1996, 39(12): 1 811–1 815.
- [11] GRILL L, CYETKO D, PETACCIA L, et al. Layer-by-layer growth of lead on Ge(1 1 1) at low temperatures[J]. *Surf. Sci.*, 2004, 562(1–3): 7–14.
- [12] YU R C, WANG W K. Formation of Ti amorphous films deposited on liquid nitrogen-cooled substrates by ion-beam sputtering[J]. *Thin Solid Films*, 1997, 302(1–2): 108–110.
- [13] BOAKEY F. Temperature dependence of the resistivity of amorphous Mn thin films [J]. *J. Non-Cryst. Solids*, 1999, 249(2–3): 189–193.
- [14] HE L, Siewenie J E. Cryogenic processing of thin metal films[J]. *Surf. Coat. Technol.*, 2002, 150(1): 76–79.
- [15] BRUNE H, RÖDER H, BORAGNO C, et al. Microscopic view of nucleation on surfaces[J]. *Phys. Rev. Lett.*, 1994, 73(14): 1 955–1 958.
- [16] BRUNE H, ROMAINEZYK C, RÖDER H, et al. Mechanism of the transition from fractal to dendritic growth of surface aggregates[J]. *Nature*, 1994, 369(6 480): 469–471.
- [17] SONG K J, CHEN W R, YEH V, et al. Morphology of ultrathin Ag films grown on Mo(111)[J]. *Surf. Sci.*, 2001, 478(1–2): 145–168.
- [18] OTOPI H. Growth of silver films on Cu (111) at low temperatures[J]. *Vacuum*, 2002, 67(2): 285–291.
- [19] SU C, YEH J C, LIN J L, et al. The growth of Ag films on a TiO<sub>2</sub> (110)-(1×1) surface[J]. *App. Sur. Sci.*, 2001, 169–170(1–2): 366–370.
- [20] SPALVINS T, BUZEK B. Frictional and morphological characteristics of ion-plated soft metallic films[J]. *Thin Solid Films*, 1981, 84(3): 267–272.
- [21] KAPAKLIS V, POULOPOULOS P, KAROUTSOS V, et al. Growth of thin Ag films produced by radio frequency magnetron sputtering[J]. *Thin Solid Films*, 2006, 510(1–2): 138–142.
- [22] WENG Lijun, SUN Jiayi, HU Ming, et al. Structure and tribological properties of Ag films deposited at low temperature [J]. *Vacuum*, 2007, 81(8): 997–1 002.
- [23] MOVCHAN B A, DEMCHISHIN A V. Study of the structure and properties of thick vacuum condensates of nickel, titanium, tungsten, aluminium oxide and zirconium dioxide[J]. *Phys. Met. Metallogr.*, 1969, 28(4): 83–90.
- [24] THORNTON J A. Influence of apparatus geometry and deposition conditions of the structure and topography of thick sputtered coatings[J]. *J. Vac. Sci. Technol.*, 1974, 11(4): 666–670.
- [25] BARNA P B, ADAMIK M. Fundamental structure forming phenomena of polycrystalline films and the structure zone models[J]. *Thin Solid Films*, 1998, 317(1–2): 27–33.
- [26] ANDERS A. A structure zone diagram including plasma-based deposition and ion etching[J]. *Thin Solid Films*, 2010, 518(15): 4 087–4 090.
- [27] ZHANG Jianmin, ZHANG Yan, XU Kewei. Dependence of stresses and strain energies on grain orientations in FCC metal films[J]. *J. Cryst. Growth*, 2005, 285(3): 427–435.
- [28] MA Fei, ZHANG Jianmin, XU Kewei. Surface-energy-driven abnormal grain growth in Cu and Ag films[J]. *App. Sur. Sci.*, 2005, 242(1–2): 55–61.
- [29] FENG Tao, JIANG Bingyao, ZHUO Sun, et al. Study on the orientation of silver films by ion-beam assisted deposition[J]. *App. Sur. Sci.*, 2008, 254(6): 1 565–1 568.

## Biographical notes

HU Ming, born in 1975, is currently an associate professor and PhD candidate at *State Key Laboratory of Solid Lubrication, Lanzhou Institute of Chemical Physics, Chinese Academy of Sciences, China*. He received his bachelor degree from *Lanzhou Institute of Chemical Physics, Chinese Academy of Sciences, China*, in 2007. His research interests include physical vapour depositing film materials and tribology.  
Tel: +86-931-4968071; E-mail: hum413@licp.cas.cn

GAO Xiaoming, born in 1978, is currently a research associate at *State Key Laboratory of Solid Lubrication, Lanzhou Institute of Chemical Physics, Chinese Academy of Sciences, China*. He received his PhD degree from *Lanzhou Institute of Chemical Physics, China*, in 2011. His study focuses on physical vapour depositing film materials.  
Tel: +86-931-4968091; E-mail: gaoxm@licp.cas.cn

SUN Jiayi, born in 1971, is currently a professor at *State Key Laboratory of Solid Lubrication, Lanzhou Institute of Chemical Physics, Chinese Academy of Sciences, China*. He got his PhD degree from *Graduate School of Chinese Academy of Sciences, China*, in 2001. His research interests include solid lubrication materials and tribology.  
Tel: +86-931-4968092; E-mail: sunjy@licp.cas.cn

WENG Lijun, born in 1966, is currently a professor at *State Key Laboratory of Solid Lubrication, Lanzhou Institute of Chemical Physics, Chinese Academy of Sciences, China*. He received his PhD degree from *Lanzhou Institute of Chemical Physics, Chinese Academy of Sciences, China* in 2007. His research interests mainly focus on physical vapor depositing coatings and their tribology.  
Tel: +86-931-4968003; E-mail: wenglj@licp.cas.cn

ZHOU Feng, born in 1976, is currently a professor at *State Key Laboratory of Solid Lubrication, Lanzhou Institute of Chemical*

*Physics, Chinese Academy of Sciences, China.* He received his PhD degree from *Lanzhou Institute of Chemical Physics, Chinese Academy of Sciences, China*, in 2004. His research interests include surfaces/interfaces of soft matters, functional coatings with extreme wetting and tunable adhesion, engineering coatings for oil seal, drag-reduction and antibiofouling, biolubrication etc. Tel: +86-931-4968466; E-mail: zhouf@licp.cas.cn

LIU Weimin, born in 1962, is currently a professor at *State Key Laboratory of Solid Lubrication, Lanzhou Institute of Chemical Physics, Chinese Academy of Sciences, China*. He received his PhD degree from *Lanzhou Institute of Chemical Physics, Chinese Academy of Sciences, China*, in 1990. His research interests include space lubrication and high performance lubricants. Tel: +86-931-4968166; E-mail: wmliu@licp.cas.cn